A MATHEMATICAL AND COMPUTATIONAL FRAMEWORK FOR MULTIFIDELITY DESIGN AND ANALYSIS WITH COMPUTER MODELS

Douglas Allaire & Karen Willcox*

Department of Aeronautics and Astronautics, 77 Massachusetts Avenue, Massachusetts Institute of Technology, Cambridge, MA 02139, USA

Original Manuscript Submitted: 02/05/2013; Final Draft Received:

A multifidelity approach to design and analysis for complex systems seeks to exploit optimally all available models and data. Existing multifidelity approaches generally attempt to calibrate low-fidelity models or replace low-fidelity analysis results using data from higher fidelity analyses. This paper proposes a fundamentally different approach that uses the tools of estimation theory to fuse together information from multifidelity analyses, resulting in a Bayesian-based approach to mitigating risk in complex system design and analysis. This approach is combined with maximum entropy characterizations of model discrepancy to represent epistemic uncertainties due to modeling limitations and model assumptions. Mathematical interrogation of the uncertainty in system output quantities of interest is achieved via a variance-based global sensitivity analysis, which identifies the primary contributors to output uncertainty and thus provides guidance for adaptation of model fidelity. The methodology is applied to multidisciplinary design optimization and demonstrated on a wing-sizing problem for a high altitude, long endurance vehicle.

KEY WORDS: *multifidelity, information fusion, sensitivity analysis, multidisciplinary design optimization*

1. INTRODUCTION

Numerical simulation tools provide essential support to all aspects of discovery and decision processes for complex systems, with applications ranging from characterization of system properties via inference, to prediction of system performance, to decision in the form of design, planning, optimization and control. For a particular application, it is often the case that engineers, scientists and decision-makers have available to them several different numerical

*Correspond to: Douglas Allaire, E-mail: dallaire@mit.edu, URL: http://web.mit.edu/dallaire/www

2152–5080/10/$35.00

models, in addition to experimental data. These numerical models may vary in "fidelity" or "skill" with respect to different quantities of interest. The models may encompass different resolutions, different physics, and different modeling assumptions. A multifidelity approach to modeling complex systems seeks to exploit optimally all available models and data. Such an approach requires systematic methods to select models with the appropriate skill for the prediction/decision task at hand. It also requires ways to synthesize information and data from different models and experiments. This paper proposes a mathematical and computational framework that lays the foundation for a multifidelity approach to modeling complex systems for design and analysis.

We propose a mathematical and computational multifidelity framework based on estimation theory. Building on the work of Ref. [1], we view the analysis or design task as a problem of Bayesian estimation, where models and experiments are used in concert to conduct a series of observations of the key parameters. If for example, the goal is optimal system design, then our task is to estimate the (unknown) optimal values of design parameters. Each model or experiment is viewed as providing a measurement that feeds into the estimation process. A Bayesian characterization of design parameters represents the level of uncertainty in each parameter at any point during the design process. Filtering methods are employed to synthesize multifidelity estimates and to evolve our estimate of the system state. Global sensitivity analysis provides a rigorous means to identify key component or subsystem contributors to uncertainty in quantities of interest for informing resource allocation decisions. The result is a multifidelity methodology that determines, with confidence, when high, medium, and low fidelity analyses are appropriate to support an analysis or design task. Further, rather than discard information as higher fidelity results become available, our approach fuses information gained from each analysis step throughout the decision process, resulting in more confident estimates of output metrics of interest.

Our approach is applicable in many different settings. For example, in modeling subsurface flows through karst aquifers, models can range from simple continuum pipe flow models [2, 3] to high-fidelity models that couple Stokes and Darcy systems [4, 5]. Climate modeling to estimate global mean temperature change in response to an emission scenario is another example where a host of different modeling options exist, such as simple climate models [6] that may consider only atmospheric effects averaged over one or more dimensions to three-dimensional atmospheric-ocean general circulation models [7]. In both cases, a rigorous approach to managing model options, their differing estimates, and their uncertainties, would better inform the decision-making process. In this paper, we demonstrate how our approach applies to the case of multifidelity modeling in the conceptual design of multidisciplinary engineering systems. Decisions made in this design phase have tremendous implications for downstream programmatic cost and schedule, as well as for the ultimate system capabilities that can be realized. Challenges arise in the conceptual design

phase because of the common use of simplified disciplinary analysis models. Indeed, according to Ref. [8], "No model is perfect. Even if there is no parameter uncertainty, so that we know the true values of all the inputs required to make a particular prediction of the process being modeled, the predicted value will not equal the true value of the process. The discrepancy is model inadequacy." It is critical that decision processes for complex systems start accounting for model inadequacy, which in this work, following Refs. [9] and [10], we refer to as *model discrepancy*.

Recent work related to the quantification of model discrepancy in engineering applications has focused on model uncertainty—uncertainty involved in selecting the best model from a set of possibilities [11]. In that body of work, model uncertainty is quantified in terms of model probabilities, which are defined as the degree of belief that a model is true, given that the true model is in the set of models considered [12]. There are many techniques for assigning model probabilities, such as expert opinion, which was incorporated in the work of Refs. [13] and [14] for nuclear safety problems; the Akaike information criterion and Bayesian information criterion discussed in Refs. [12] and [15]; and a Bayesian statistical framework proposed in Ref. [11] based on comparing experimental data to model outcomes. Once model probabilities have been assigned, it is common to fuse estimates from the various models through techniques of the adjustment factors approach [14], and Bayesian model averaging [16].

This previous work on quantification of model uncertainty assigns a model probability to each model in the selection set, to encompass the degree of belief of each model relative to the other models. Our approach differs in that we assign a probability distribution to the output of each individual model, on the basis of the model discrepancy associated with that particular model. Our approach also differs in that we fuse information from various modeling sources with the tools of Bayesian inference, where it is implied that each model yields some quantity of information that, regardless of fidelity level, leads to better estimates in terms of diminished variance. This is not the case for the methods of Bayesian model averaging and the adjustment factors approach, where it is common for the estimate arrived at through fusing information from several models to have a larger variance than the estimates from the individual models alone.

Model discrepancy present in decision-making processes leads to risk in the form of variance in estimates of quantities of interest (e.g., quantities related to system performance, cost or schedule). Our goal is to mitigate this risk by providing a systematic means of managing and fusing information from different available modeling options. There is a wide body of work related to quantification of risk in probabilistic terms, particularly in the nuclear engineering community, where considerable efforts are put into the probabilistic risk assessment of complex nuclear facilities that began with the work of Ref. [17]. Probabilistic risk assessment generally defines risk on the basis of severity of a failure event and how likely that event is to occur. Our view of risk, particularly in the context of conceptual

design where we may be more concerned about performance estimates than the occurrence of rare failure events, is more inline with the views of the financial engineering community, where risk has been viewed as being directly proportional to the variance of a quantity of interest outcome, such as in mean-variance optimization of modern portfolio theory [18]. Quantifying and subsequently mitigating this type of risk is critical in conceptual design, where the goal is to minimize risk in the selection of a particular system architecture or architectures with which to proceed to the preliminary design phase.

Our approach begins with defining a design or analysis case of interest, followed by the analysis of that case by a model whose model discrepancy has been quantified. This then allows us to assess risk in terms of the variance of an output quantity of interest. We employ methods of Bayesian inference and global sensitivity analysis to reduce this variance by systematically incorporating higher fidelity models in the design process. We set up this problem in Section 2. Our approach and background material on each component of it is developed in Section 3. A discussion of the application of our methodology to multidisciplinary design optimization and the results of applying our approach to a wing-sizing problem for an aerospace vehicle are presented in Section 4. Conclusions and future work are discussed in Section 5.

2. PROBLEM SETUP

Throughout this work, for clarity of the exposition, we will consider a system consisting of two subsystems. However, the methods developed here can be extended to any number of subsystems. We denote the two subsystems as A and B. For each subsystem, we have a set of modeling options available, which we denote as $\mathcal{A}$ and $\mathcal{B}$ for subsystems A and B respectively. Each modeling choice for each subsystem is responsible for estimating a vector of quantities denoted as $\mathbf{q}_{\mathcal{A}} \in \mathbb{R}^{o_{\mathcal{A}}}$, where $o_{\mathcal{A}}$ is the number of outputs of subsystem A, and $\mathbf{q}_{\mathcal{B}} \in \mathbb{R}^{o_{\mathcal{B}}}$, where $o_{\mathcal{B}}$ is the number of outputs of subsystem B. The ith modeling choice employed for each subsystem during a design or analysis process is written as $\mathcal{A}_i$ and $\mathcal{B}_i$, where $i \in \{1, 2, \ldots, K\}$ and $K \geq 1$. For modeling choice $\mathcal{A}_i$ for subsystem A, we estimate $\mathbf{q}_{\mathcal{A}_i}$ as $\mathbf{Q}_{\mathcal{A}_i}(\mathbf{d}_{\mathcal{A}_i}) = g_{\mathcal{A}_i}(\mathbf{d}_{\mathcal{A}_i}) + \epsilon_{\mathcal{A}_i}(\mathbf{d}_{\mathcal{A}_i})$, where $\mathbf{d}_{\mathcal{A}_i}$ are the inputs to modeling choice $\mathcal{A}_i$, $\mathbf{d}_{\mathcal{A}_i} \in \mathbb{R}^{k_{\mathcal{A}_i}}$, where $k_{\mathcal{A}_i}$ is the number of inputs to subsystem model $\mathcal{A}_i$, $\epsilon_{\mathcal{A}_i}(\mathbf{d}_{\mathcal{A}_i})$ is a stochastic process representing the discrepancy in source $\mathcal{A}_i$, and $g_{\mathcal{A}_i} : \mathbb{R}^{k_{\mathcal{A}_i}} \rightarrow \mathbb{R}^{o_{\mathcal{A}}}$. Similarly for modeling choice $\mathcal{B}_i$ for subsystem B we estimate $\mathbf{q}_{\mathcal{B}_i}$ as $\mathbf{Q}_{\mathcal{B}_i}(\mathbf{d}_{\mathcal{B}_i}) = g_{\mathcal{B}_i}(\mathbf{d}_{\mathcal{B}_i}) + \epsilon_{\mathcal{B}_i}(\mathbf{d}_{\mathcal{B}_i})$, where $\mathbf{d}_{\mathcal{B}_i}$ are the inputs to modeling choice $\mathcal{B}_i$, $k_{\mathcal{B}_i}$ is the number of inputs to subsystem model $\mathcal{B}_i$, $\mathbf{d}_{\mathcal{B}_i} \in \mathbb{R}^{k_{\mathcal{B}_i}}$, $\epsilon_{\mathcal{B}_i}(\mathbf{d}_{\mathcal{B}_i})$ is a stochastic process representing the discrepancy in source $\mathcal{B}_i$, and $g_{\mathcal{B}_i} : \mathbb{R}^{k_{\mathcal{B}_i}} \rightarrow \mathbb{R}^{o_{\mathcal{B}}}$.

We define the vector of outputs from the modeling choices of the two subsystems as $\mathbf{z}_i$, where $\mathbf{z}_i = (\mathbf{q}_{\mathcal{A}_i}, \mathbf{q}_{\mathcal{B}_i})^T$.

A system level scalar quantity of interest c, is then estimated as $C = f_{\mathcal{M}_i}(\mathbf{Z}_i) + \epsilon_{\mathcal{M}_i}(\mathbf{Z}_i)$, where $\mathcal{M}_i = \{\mathcal{A}_i, \mathcal{B}_i\} \subset \mathcal{A} \times \mathcal{B}$ is the system level modeling choice at the ith iteration comprising a selection of a modeling option for each subsystem, $\epsilon_{\mathcal{M}_i}(\mathbf{Z}_i)$ is a stochastic process representing the discrepancy in $f_{\mathcal{M}_i}(\mathbf{Z}_i)$, $f_{\mathcal{M}_i}(\mathbf{Z}_i) : \mathbb{R}^{k_{\mathcal{A}_i} k_{\mathcal{B}_i}} \rightarrow \mathbb{R}$, and $\mathbf{Z}_i = (\mathbf{Q}_{\mathcal{A}_i}, \mathbf{Q}_{\mathcal{B}_i})^T$. In this work we do not consider other options for estimating c from $\mathbf{z}$ and focus instead on the choices to be made at the subsystem level. The result of exercising a modeling choice, $\mathcal{M}_i$, is a conditional distribution $p(c|\mathbf{d}_{\mathcal{M}_i}, \mathcal{M}_i)$, where $\mathbf{d}_{\mathcal{M}_i} = (\mathbf{d}_{\mathcal{A}_i}, \mathbf{d}_{\mathcal{B}_i})^T$.

In general we may have many different subsystems or disciplines in a system of interest, each of which may have available many different modeling options. The goal of our multifidelity approach is to find a search algorithm, or policy, that optimally chooses when to use a particular modeling option, given some objective function. If we denote the modeling option employed at time t (here time indexes each time a model choice is made, e.g., the first modeling choice occurs at $t = 1$, the second at $t = 2$, etc.) as $\mathcal{M}_t$, then at time t we have a history set $\mathcal{H}_t = \{(\mathcal{M}_1, \mathbf{d}_{\mathcal{M}_1}), \ldots, (\mathcal{M}_t, \mathbf{d}_{\mathcal{M}_t})\}$. A search algorithm can then be defined as a policy, $\pi(\mathcal{M}_{t+1}|\mathcal{H}_t)$, that maps a given history set to the next modeling option to be employed.

The particular objective we consider here focuses on maximizing the expected variance reduction in a given quantity of interest at each successive modeling choice stage. Assuming we are at time t, our current quantity of interest variance is given as $\text{var}(C|\mathbf{d}_{\mathcal{M}_t}, \mathcal{M}_t)$, where $C|\mathbf{d}_{\mathcal{M}_t}, \mathcal{M}_t \sim p(c|\mathbf{d}_{\mathcal{M}_t}, \mathcal{M}_t)$. Under a particular policy $\pi(\mathcal{M}_{t+1}|\mathcal{H}_t)$, the expected variance of our quantity of interest at time $t+1$ is given as $\mathbb{E}[\text{var}(C|\mathbf{d}_{\mathcal{M}_{t+1}}, \mathcal{M}_{t+1})$. We consider an expectation of the variance here because we may not know in advance the discrepancy associated with modeling choice $\mathcal{M}_{t+1}$ and we may also not know the values of $\mathbf{d}_{\mathcal{M}_{t+1}}$ at which the models will be evaluated. The expected variance reduction, $\mathcal{R}$, is then given as

$$\mathcal{R}(\pi(\mathcal{M}_{t+1}|\mathcal{H}_t)) = \text{var}(C|\mathbf{d}_{\mathcal{M}_t}, \mathcal{M}_t) - \mathbb{E}[\text{var}(C|\mathbf{d}_{\mathcal{M}_{t+1}}, \mathcal{M}_{t+1})]. \tag{1}$$

Thus, we wish to find a policy $\pi^*(\mathcal{M}_{t+1}|\mathcal{H}_t)$ where

$$\pi^*(\mathcal{M}_{t+1}|\mathcal{H}_t) = \arg\max_{\pi \in \Pi} \mathcal{R}(\pi(\mathcal{M}_{t+1}|\mathcal{H}_t)), \tag{2}$$

where Π is the set of admissible policies. Here we assume that the policy is initialized by a prescribed first modeling choice, $\mathcal{M}_1$.

3. APPROACH

To manage multifidelity models by finding an optimal policy according to (2), we must have a means for estimating the discrepancy associated with a modeling option. Once we have estimated the discrepancy we must estimate the expected variance reduction under a particular policy, as given by (1). For this, we need to be able to apportion the variance of a given to quantity among its contributing factors. In the following subsections we discuss our discrepancy quantification procedure, as well as how we approach variance apportionment. Following that we present our optimal policy for selecting the next modeling option. We conclude this section with some considerations of model fusion opportunities and a step-by-step procedure for model management and information synthesis in multifidelity engineering tasks.

3.1 Quantification of Model Discrepancy

Mathematical models of reality implemented in computer codes contain many different sources of uncertainty. Among these are parameter uncertainty, residual variability, parametric variability, observation error, code uncertainty, and model discrepancy [8]. Following Ref. [8], parameter uncertainty relates to uncertainty associated with the values of model inputs; residual variability relates to the variation of a particular process outcome even when the conditions of that process are fully specified, parametric variability results when certain inputs require more detail than is desired (or possible) and are thus left unspecified in the model; observation error involves the use of actual observations in a model calibration process; code uncertainty results when a code is so complex or computationally involved that it may not be possible to execute the code at every possible input configuration of interest, thus there is some additional uncertainty related to regions of the input space that have not been interrogated; and model discrepancy relates to the fact that no model is perfect, and thus some aspects of reality may have been omitted, improperly modeled, or contain unrealistic assumptions.

The work presented here focuses entirely on model discrepancy and how it relates to model fidelity. We propose an association between high model discrepancy, quantified in terms of model output variance, with low model fidelity. Thus, as model discrepancy is reduced, model fidelity increases. While there are many different ways of viewing what is meant by model fidelity, the connection with model discrepancy we propose here provides us with a readily quantifiable notion of fidelity that permits us to incorporate probabilistic methods of Bayesian inference and global sensitivity analysis for information synthesis and fidelity management.

To establish a probabilistic representation of model discrepancy requires a means of producing probability distributions from uncertainty information. This is because characterizations of uncertainty with probability distributions

are rarely constructed from complete uncertainty information. Instead, these characterizations are inferred in some way from available information. In some cases, a great deal of information regarding the outcome of a particular experiment (e.g., rolling a fair die or tossing a fair coin) may be had, and thus probability distributions may be assigned with confidence. In most cases, however, such complete uncertainty information is not available (e.g., any form of epistemic uncertainty, where epistemic uncertainty is uncertainty that derives from imperfect knowledge rather than any intrinsic variability). However, it may still be desirable, or even critical, that particular quantities, such as the likelihood of some event's occurrence, be estimated. According to Ref. [19], information entropy provides a constructive criterion for assigning probability distributions on the basis of incomplete uncertainty information, and distributions assigned by maximizing information entropy are maximally noncommittal with regard to missing information. Thus, in this work we assign to epistemic uncertainties probability distributions that maximize information entropy.

We create maximum entropy distributions for the model discrepancy of some model $\mathcal{M}_i$ that is used to estimate some real-world quantity z^* as follows. Let the estimate of z^* from the model be z_i. First, following Ref. [20], we note that qualitatively, $|z^* - z_i|$ should not be too large, otherwise we would not consider using model $\mathcal{M}_i$. Given this information, we assign a normalized prior density to estimate the real-world quantity z^* in the form

$$p(z^*) = \sqrt{\frac{\omega_{Z_i}}{2\pi}} \exp\left[-\frac{\omega_{Z_i}}{2}(z^* - z_i)^2\right], \tag{3}$$

where ω_{Z_i} is a weight parameter for model choice $\mathcal{M}_i$. Qualitatively, (3) states that we believe it is unlikely that $|z^* - z_i|$ is much greater than $1/\sqrt{\omega_{Z_i}}$ [20]. Quantitatively, (3) states that we believe $\mathbb{P}(|Z - z_i| < 1/\sqrt{\omega_{Z_i}}) > 0.68$, $\mathbb{P}(|Z - z_i| < 2/\sqrt{\omega_{Z_i}}) > 0.95$, and $\mathbb{P}(|Z - z_i| < 3/\sqrt{\omega_{Z_i}}) > 0.99$, where Z is a random variable with density $p(z^*)$. The assignment of this probability density requires the specification of the weight parameter ω_{Z_i}. This can be done by providing to an expert the model estimate, z_i, as well as the conditions under which the model was run to arrive at the estimate. The expert can then provide information relating to the uncertainty associated with the estimate. This information can be in the form of a percentage of z_i, denoted γ, or an absolute quantity, denoted δ, giving the range of the true z^* (according to the expert) as either $z_i \pm \gamma z_i$ or $z_i \pm \delta$. Based on this expert input, a value can then be assigned to ω_{Z_i}, and the maximum entropy distribution for z^* given this information is given by Equation 3. For a conservative estimate, the weight parameter can be set as $1/\sqrt{\omega_{Z_i}} = \delta$ or $1/\sqrt{\omega_{Z_i}} = \gamma z_i$. For an aggressive estimate of the uncertainty, the weight parameter can be set according to $1/\sqrt{\omega_{Z_i}} = \delta/3$ or $1/\sqrt{\omega_{Z_i}} = \gamma z_i/3$. We assume in this work that our experts provide reasonable estimates for the range of the true quantities being elicited. Forming consensus distributions from information elicited from several experts could be employed to relax this assumption as

discussed in Ref. [21], where a method for determining both the probabilistic and technical abilities of the experts is also developed. The technical abilities of the expert are assessed by comparing their opinions to relevant historical data or experiments. This information can be used to calibrate the experts as part of a weight determination process in forming a consensus distribution from a weighted average of individual expert elicited distributions. Experts that are trusted more on the basis of their probabilistic and technical abilities are assigned larger weights.

As shown in Equation 3, we are considering only normal distributions in the suggested elicitation process. From an information theory perspective, this is the most reasonable distribution given the information we are eliciting. If more information were gathered, such as support bounds for model outputs or known bias, then this information could be included in the construction of the model discrepancy distributions. However, more formal elicitation processes are beyond the scope of this work.

3.2 Variance Apportionment

The goal of this work is to determine how to systematically manage levels of model fidelity according to (2). To achieve this goal we utilize a method of variance apportionment known as global sensitivity analysis. Global sensitivity analysis is a rigorous means for apportioning model output variance among model factors. The objective of the method is shown in Figure 1, where the pie represents the variance in a model output, which is then decomposed according to factor contributions. To achieve this decomposition, following Ref. [22], we consider a function

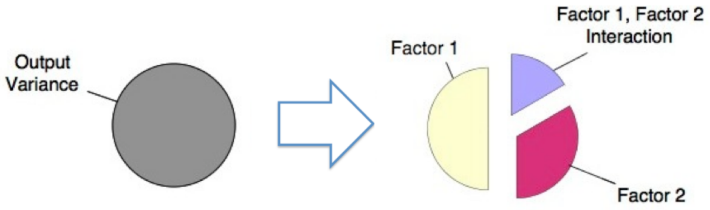

FIG. 1: Apportioning Output Variance

$f(\mathbf{z}) = f(z_1, z_2, \ldots, z_m) \in \mathbb{R}$ defined on the unit hypercube $I^m = \{(z_1, z_2, \ldots, z_m) : 0 \leq z_i \leq 1, i = 1, 2, \ldots, m\}$, where $f(\mathbf{z})$ belongs to a vector space $\mathcal{Z}$. Let $(I^m, \mathcal{B}(I^m), \mu)$ be a measure space, where $\mathcal{B}(I^m)$ denotes the Borel σ-field on I^m and μ is a measure on $\mathcal{B}(I^m)$, and let $\mathcal{Z}$ consist of all integrable functions with respect to μ. Further, let μ be a product measure, $\mathrm{d}\mu(\mathbf{z}) = \mathrm{d}\mu(z_1, \ldots, z_m) = \prod_{i=1}^m \mathrm{d}\mu_i(z_i)$, with unit mass and a density defined as $p(\mathbf{z}) = \mathrm{d}\mu(\mathbf{z})/\mathrm{d}\mathbf{z} = \prod_{i=1}^m p_i(z_i)$, where $p_i(z_i)$ is the marginal density of z_i. The inner product $\langle \cdot, \cdot \rangle : \mathcal{Z} \times \mathcal{Z} \to \mathbb{R}$ induced by μ is given as

$$\langle f, g \rangle = \int_{I^m} f(\mathbf{z}) g(\mathbf{z}) \mathrm{d}\mu(\mathbf{z}), \tag{4}$$

where $f(\mathbf{z}), g(\mathbf{z}) \in \mathcal{Z}$.

We may decompose $\mathcal{Z}$ into subspaces defined as

$$\begin{aligned}
\mathcal{V}_0 &:= \{f \in \mathcal{Z} : f = C, \text{ where } C \in \mathbb{R} \text{ is a constant}\},\\
\mathcal{V}_i &:= \{f \in \mathcal{Z} : f = f_i(z_i) \text{ is a univariate function and } \int_{I^1} f_i(z_i)\mathrm{d}\mu_i(z_i) = 0\},\\
\mathcal{V}_{ij} &:= \{f \in \mathcal{Z} : f = f_{ij}(z_i, z_j) \text{ is a bivariate function and } \int_{I^1} f_{ij}(z_i, z_j)\mathrm{d}\mu_k(z_k) = 0, k = i, j\},\\
&\vdots\\
\mathcal{V}_{i_1,\ldots,i_s} &:= \{f \in \mathcal{Z} : f = f_{i_1,\ldots,i_s}(z_{i_1}, \ldots, z_{i_s}) \text{ is an } s\text{-variate function and}\\
&\qquad \int_{I^1} f_{i_1,\ldots,i_s}(z_{i_1}, \ldots, z_{i_s})\mathrm{d}\mu_k(z_k) = 0, k = i_1, \ldots, i_s\},\\
&\vdots\\
\mathcal{V}_{12\ldots m} &:= \{f \in \mathcal{Z} : f = f_{12\ldots m}(z_1, z_2, \ldots, z_m) \text{ is an } m\text{-variate function and}\\
&\qquad \int_{I^1} f_{12\ldots m}(z_1, z_2, \ldots, z_m)\mathrm{d}\mu_k(z_k) = 0, k = 1, 2, \ldots, m\}. \qquad (5)
\end{aligned}$$

Any two functions, $f_{i_1,\ldots,i_s}(z_{i_1}, \ldots, z_{i_s}), f_{j_1,\ldots,j_p}(z_{j_1}, \ldots, z_{j_p})$, with at least one index differing are orthogonal

$$\left\langle f_{i_1,\ldots,i_s}, f_{j_1,\ldots,j_p} \right\rangle = 0. \qquad (6)$$

As shown by Ref. [22], we may write $\mathcal{Z}$ as the direct sum of the subspaces defined above,

$$\mathcal{Z} = \mathcal{V}_0 \oplus \sum_i \mathcal{V}_i \oplus \sum_{i<j} \mathcal{V}_{ij} \oplus \cdots \oplus \sum_{i_1<i_2<\cdots<i_s} \mathcal{V}_{i_1 i_2 \ldots i_s} \oplus \cdots \oplus \mathcal{V}_{12\ldots m}, \qquad (7)$$

which is often written more compactly as [23]

$$\mathcal{Z} = \bigoplus_{\mathbf{u} \subseteq \mathcal{I}} \mathcal{V}_{\mathbf{u}}, \qquad (8)$$

where $\mathcal{I} := \{1, 2, \ldots, m\}$ denotes the set of coordinate indices and $\mathcal{V}_\emptyset = \mathcal{V}_0$. As a result, we may write $f(\mathbf{z}) \in \mathcal{Z}$ as

$$f(\mathbf{z}) = f_0 + \sum_i f_i(z_i) + \sum_{i<j} f_{ij}(z_i, z_j) + \cdots + f_{12\ldots m}(z_1, z_2, \ldots, z_m) = \sum_{\mathbf{u} \subseteq \mathcal{I}} f_{\mathbf{u}}(\mathbf{z}_{\mathbf{u}}), \qquad (9)$$

where $f_\emptyset(\mathbf{z}_\emptyset) = f_0$. The representation of $f(\mathbf{z})$ given in Equation 9 is referred to as the high dimensional model representation (HDMR) and is unique up to the choice of the measure μ.

For global sensitivity analysis, we specify the measure μ as the ordinary Lebesgue measure and let $\mathcal{Z}$ be defined as the space of square-integrable functions on I^m, $\mathcal{Z} := \mathcal{L}_2(I^m, \mathcal{B}(I^m), \mu)$. If z_i are assumed to be uniform random variables Z_i, then we may square and integrate Equation 9 and write the overall variance of $f(\mathsf{Z})$ (where $\mathsf{Z} = [Z_1, Z_2, \ldots, Z_m]^T$) as

$$\text{var}(f(\mathsf{Z})) = \sum_i V_i + \sum_{i<j} V_{ij} + \cdots + V_{12\ldots m} = V, \tag{10}$$

where individual variances are given by

$$V_{i_1,\ldots,i_s} := \text{var}(f_{i_1,\ldots,i_s}(Z_{i_1}, \ldots, Z_{i_s})) = \int_{I^s} (f_{i_1,\ldots,i_s}(Z_{i_1}, \ldots, Z_{i_s}))^2 \mathrm{d}z_{i_1} \ldots \mathrm{d}z_{i_s}. \tag{11}$$

The variance decomposition given by Equation 10 is precisely the qualitative notion depicted in Figure 1. Main effect global sensitivity indices are then defined as

$$S_{i_1,\ldots,i_s} := \frac{V_{i_1,\ldots,i_s}}{V}. \tag{12}$$

Calculation of these indices may be carried out in many ways, such as a Monte Carlo simulation approach known as the Sobol' method as shown in Ref. [24], a Fourier analysis based approach as shown in Ref. [25], a polynomial chaos expansion based approach as shown in Ref. [26], and a sparse grid based approach as shown in Ref. [27].

3.3 A Model Management Policy

To construct an optimal policy according to (2), we first must consider what modeling options might be available at any given time during a design or analysis task. Consider a system comprised of two subsystems, A and B as before. For each subsystem we have a "low-fidelity" modeling option A^{LO} and B^{LO} respectively, and the potential to obtain or construct a higher fidelity modeling option A^{HI} and B^{HI} respectively. In this work we do not explicitly include the cost of obtaining or constructing a modeling option, or the cost of using that option. Instead, we assume that fidelity level can only be incremented one level at a time for one subsystem at a time. The explicit inclusion of cost in the problem setup is a topic of future work. The progression from low-fidelity models to higher fidelity models one step at a time is a typical practice and our aim here is to identify how to optimally perform that progression.

Assume that we have run the low-fidelity modeling option $\mathcal{M}_1 = \{A^{\text{LO}}, B^{\text{LO}}\}$, and that subsystem A again estimates the vector of quantities $\mathbf{a}$ and subsystem B estimates the vector of quantities $\mathbf{b}$. Our quantity of interest is c and is a function of $\mathbf{a}$ and $\mathbf{b}$. Our task is to determine which higher fidelity modeling option, A^{HI} or B^{HI} we

should incorporate next. According to (2), the optimal selection will be the subsystem for which we obtain the largest expected variance reduction in the quantity of interest when the fidelity of that subsystem is incremented. For subsystem A, the expected variance reduction is given as

$$\mathcal{R}(\mathcal{M}_2 = \{A^{\text{HI}}, B^{\text{LO}}\}) = \text{var}(C|\mathbf{d}_{\mathcal{M}_1}) - \mathbb{E}[\text{var}(C|\mathbf{d}_{\mathcal{M}_2})], \tag{13}$$

and the current amount of variance of C that subsystem A is contributing is given as

$$\mathcal{S}_{\mathbf{a}}\text{var}(C|\mathbf{d}_{\mathcal{M}_1}) = \sum_{\mathbf{a}\subseteq\mathcal{D}_{A_1}} S_{\mathbf{a}}\text{var}(C|\mathbf{d}_{\mathcal{M}_1}). \tag{14}$$

We know qualitatively that A^{HI} is of higher fidelity than A^{LO}, and thus, we believe we will have a better estimate of the quantities $\mathbf{a}$. Therefore, we will achieve between 0 and $\mathcal{S}_{\mathbf{a}}\text{var}(C|\mathbf{d}_{\mathcal{M}_1})$ reduction of variance by incorporating choice A^{HI} next. We capture this by introducing a parameter $\alpha_{\mathbf{a}}$, where $0 \leq \alpha_{\mathbf{a}} \leq 1$, and writing the expected variance reduction as

$$\mathcal{R}(\mathcal{M}_2 = \{A^{\text{HI}}, B^{\text{LO}}\}) = \alpha_{\mathbf{a}}\mathcal{S}_{\mathbf{a}}\text{var}(C|\mathbf{d}_{\mathcal{M}_1}). \tag{15}$$

Similarly, we may write the expected variance reduction when B^{HI} is incorporated next as

$$\mathcal{R}(\mathcal{M}_2 = \{A^{\text{LO}}, B^{\text{HI}}\}) = \alpha_{\mathbf{b}}\mathcal{S}_{\mathbf{b}}\text{var}(C|\mathbf{d}_{\mathcal{M}_1}), \tag{16}$$

where $0 \leq \alpha_{\mathbf{b}} \leq 1$. If $\alpha_{\mathbf{a}}\mathcal{S}_{\mathbf{a}} > \alpha_{\mathbf{b}}\mathcal{S}_{\mathbf{b}}$, then the expected variance reduction that would result from incorporating A^{HI} is larger than that expected from incorporating B^{HI}. If we have information about the higher fidelity modeling options, we can incorporate it by assigning distributions to the $\alpha_{\mathbf{a}}$ and $\alpha_{\mathbf{b}}$ terms. Assuming in this work that we have no further information about the higher fidelity options, we assume that $\alpha_{\mathbf{a}} = \alpha_{\mathbf{b}}$. Then at any stage in a multifidelity design or analysis task, according to (2) and the restriction to incrementing one fidelity level at a time for one subsystem at a time, the optimal policy is to increment the fidelity of the subsystem with the largest sensitivity index.

3.4 Information Fusion

In complex system analysis and design processes it is typical to discard information gained from lower fidelity models once information from higher fidelity models has been obtained. In the example of the previous subsection, once we

run say $\{A^{\text{HI}}, B^{\text{LO}}\}$ the results from $\{A^{\text{LO}}, B^{\text{LO}}\}$ may be discarded. Here we take a different approach and consider fusing the information gained from every source. In the language of estimation theory, we view the outputs (with associated model discrepancy) calculated from each modeling choice as measurements that can be used to estimate the true output. That is, for each model $\mathcal{M}_i$, we have a measurement $Z_i|\mathbf{d}_{\mathcal{M}_i}$. Here we work with a single quantity and note that the process developed here can be applied to all outputs of the models. We denote the true (unknown) output as z^*. In order to obtain the best possible estimate of z^*, we wish to use not just the last, but all of the possible measurements, $Z_1|\mathbf{d}_{\mathcal{M}_t}, Z_2|\mathbf{d}_{\mathcal{M}_t}, \ldots, Z_t|\mathbf{d}_{\mathcal{M}_t}$, where here we assume the input spaces for each modeling option are the same to ensure we are fusing information for the same input configuration. How to deal with the situation where the input spaces for the modeling choices differ is a topic of future work.

The information fusion takes place via a Bayesian updating process. Following Ref. [28], we treat the distribution associated with the model outputs as a likelihood function and assume a diffuse uniform prior. Thus, our posterior density of z^* given the t model measurements is

$$p(z^*|\{Z_1|\mathbf{d}_{\mathcal{M}_t}, Z_2|\mathbf{d}_{\mathcal{M}_t}, \ldots, Z_t|\mathbf{d}_{\mathcal{M}_t}\}) \propto L(z^* - z_1|\mathbf{d}_{\mathcal{M}_t}, z^* - z_2|\mathbf{d}_{\mathcal{M}_t}, \ldots, z^* - z_t|\mathbf{d}_{\mathcal{M}_t}), \tag{17}$$

where $L(\cdot, \cdot, \ldots, \cdot)$ is the likelihood function. Since our model discrepancy procedure developed in Section 3.1 results in normal distributions for each measurement, we may analytically update mean and variance information for z^* as new models are exercised. If our model discrepancy were quantified in a manner that resulted in arbitrary distributions, then the posterior density would still be given by Equation 17, however, this could result in the need for expensive sampling based procedures such as Markov chain Monte Carlo to obtain samples of the posterior. The specification of an arbitrary joint distribution among dependent model discrepancies terms for several models would also be a challenging task. Thus, here we assume our model discrepancy terms are always normally distributed. In the following two paragraphs we demonstrate how this assumption allows us to update mean and variance information for two cases. First, we consider the case of known correlation between models, and second, we consider the case of unknown correlation between models.

Correlations in models of different fidelity levels are expected to exist owing to the fact that the same physics may be used to model certain phenomena in different models and similar data sets may have been used to calibrate any empirical aspects of the models. The correlation manifests itself in the discrepancy of each model output when compared to reality. Given that similar physics and information are employed in some models, it is likely that the errors these models make in estimating reality be correlated. If we assume the correlations are known from historical

data, then following Ref. [28], we may write the posterior for z^* as

$$p(z^*|\{Z_1|\mathbf{d}_{\mathcal{M}_t}, Z_2|\mathbf{d}_{\mathcal{M}_t}, \ldots, Z_t|\mathbf{d}_{\mathcal{M}_t}\}) = \frac{1}{\sqrt{2\pi \text{ var}(Z^*)}} \exp\left(-\frac{(z^* - \mathbb{E}[Z^*])^2}{2 \text{ var}(Z^*)}\right), \tag{18}$$

where

$$\mathbb{E}[Z^*] = \frac{\mathbf{e}^T\Sigma^{-1}\mathbf{z}_{1:t}}{\mathbf{e}^T\Sigma^{-1}\mathbf{e}} \tag{19}$$

$$\text{var}(Z^*) = \frac{1}{\mathbf{e}^T\Sigma^{-1}\mathbf{e}}, \tag{20}$$

$\mathbf{e} = (1, \ldots, 1)^T$, $\mathbf{z}_{1:t} = [z_1|\mathbf{d}_{\mathcal{M}_t}, z_2|\mathbf{d}_{\mathcal{M}_t}, \ldots, z_t|\mathbf{d}_{\mathcal{M}_t}]^T$ and Σ is the covariance matrix. Letting $\sigma_i^2 = \text{var}(Z_i|\mathbf{d}_{\mathcal{M}_t})$ and ρ_{ij} be the correlation between modeling options i and j, the covariance matrix is written as

$$\Sigma = \begin{pmatrix} \sigma_1^2 & \rho_{12}\sigma_1\sigma_2 & \cdots & \rho_{1t}\sigma_1\sigma_t \\ \rho_{21}\sigma_2\sigma_1 & \sigma_2^2 & \cdots & \rho_{2t}\sigma_2\sigma_t \\ \vdots & \vdots & \ddots & \vdots \\ \rho_{t1}\sigma_t\sigma_1 & \rho_{t2}\sigma_t\sigma_2 & \cdots & \sigma_t^2 \end{pmatrix}$$

To demonstrate this approach, assume we have outputs from two models that we wish to fuse, $Z_1|\mathbf{d}_{\mathcal{M}_2}$ and $Z_2|\mathbf{d}_{\mathcal{M}_2}$. Then the fused estimate, Z^*, is a normally distributed random variable with mean

$$\mathbb{E}[Z^*] = \frac{(\sigma_2^2 - \rho_{12}\sigma_1\sigma_2)z_1|\mathbf{d}_{\mathcal{M}_2} + (\sigma_1^2 - \rho_{12}\sigma_1\sigma_2)z_2|\mathbf{d}_{\mathcal{M}_2}}{\sigma_1^2 + \sigma_2^2 - 2\rho_{12}\sigma_1\sigma_2}, \tag{21}$$

and variance

$$\text{var}(Z^*) = \frac{(1 - \rho_{12}^2)\sigma_1^2\sigma_2^2}{\sigma_1^2 + \sigma_2^2 - 2\rho_{12}\sigma_1\sigma_2}. \tag{22}$$

Fused estimates Z^* are shown in Figure 2 for several different correlation cases. The figure reveals how the Bayesian update combines information and also demonstrates that accounting for correlations is critical. The top three plots in the figure demonstrate how information from similar models is fused. On the far left, the models are assumed to be uncorrelated and the updated estimate has smaller variance and an averaged mean from the two sources. As we move to the right, the correlation between the information sources increases, which increases the variance of the fused estimate (as can be seen by the diminished height of the probability density function) and pushes the fused estimate in the direction of the information source with the lower model discrepancy. This can be seen clearly on the rightmost

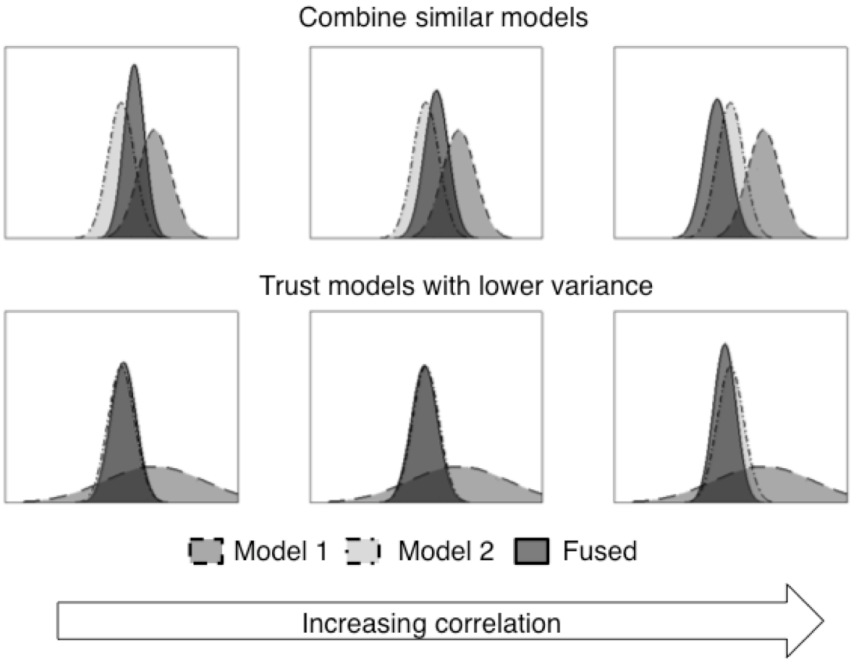

FIG. 2: Examples of the resultant fused probability densities given two initial densities to be fused. The top three plots fuse information from similar models while the bottom three plots fuse information from a high fidelity and low fidelity model. The correlation between models is increasing from left to right in the figure.

plot, where the fused estimate is actually to the left of either of the two previous estimates. This can be explained by considering that highly correlated estimates are more likely to both be on the same side of the true quantity (e.g., either both to the left or both to the right), and therefore the updating procedure pushes the new estimate towards the information source in which we have most confidence, since that estimate is more likely to be closer to the true value of the quantity being estimated. The bottom three plots in the Figure 2 demonstrate how the higher fidelity model is trusted more when one of the models is considerably more inadequate. On the far left, the models are again assumed to be uncorrelated and the updated estimate is very nearly the same as the estimate from the higher fidelity information source, though again, the variance of the combined estimate is less than either of the two previous estimates. As we move to the right, the correlation between the sources of information increases, which again increases the variance of the fused estimate and pushes the fused estimate in the direction of the higher fidelity model estimate. However, for this case, as we move to the far right plot and high correlation, instead of increasing, the variance of the fused estimate actually decreases, as can be seen by the increased height of the probability density function of the fused estimate as compared with the middle plot. This can be explained by considering that in this plot we have assumed a high correlation between a high fidelity model and a very low fidelity model, which suggests that the adequacy of our low

fidelity model has been understated (since it is so highly correlated with a model in which we have great confidence), and thus the low fidelity model is providing us with more information than its level of fidelity implies.

While it is likely that models are correlated, we may not know the covariance matrix Σ. For this situation, following Ref. [28], we recommend assuming an inverse Wishart density as a prior for Σ,

$$p(\Sigma) \propto |\Sigma^{-1}|^{(\delta+2t)/2} \exp(-\delta \text{tr}[\Sigma^{-1}\Sigma_0]/2), \tag{23}$$

where Σ_0 is a symmetric positive definite matrix constructed by using data from δ sources (e.g., experts) that contains initial estimates of the entries of the true covariance matrix. Assuming an inverse Wishart distribution for the covariance results in a posterior density for z^* of

$$p(z^*|\{Z_1|\mathbf{d}_{\mathcal{M}_t}, Z_2|\mathbf{d}_{\mathcal{M}_t}, \ldots, Z_t|\mathbf{d}_{\mathcal{M}_t}\}) \propto \left(\frac{1+(z^*-\mathbb{E}[Z^*])^2}{(\delta+t-3)\text{var}(Z^*)}\right)^{-(\delta+t)/2}, \tag{24}$$

where

$$\mathbb{E}[Z^*] = \frac{\mathbf{e}^T\Sigma_0^{-1}\mathbf{z}_{1:t}}{\mathbf{e}^T\Sigma_0^{-1}\mathbf{e}} \tag{25}$$

$$\text{var}(Z^*) = \frac{\delta + (\mathbb{E}[Z^*]-\mathbf{z}_{1:t})^T\Sigma_0^{-1}\mathbf{z}_{1:t}}{(\delta+t-3)\mathbf{e}\Sigma_0^{-1}\mathbf{e}}. \tag{26}$$

Under these assumptions, the posterior distribution of z^* is a Student's t-distribution with $\delta+t-1$ degrees of freedom.

3.5 Algorithm

We now establish an algorithm for fidelity management and information synthesis that incorporates the tools of global sensitivity analysis and model fusion. First, we select a modeling choice and design or analysis case to analyze. Next we quantify the uncertainty in system outputs caused by model discrepancy of the component models employed in the design or analysis process. Once this uncertainty is quantified, we fuse information from previously exercised modeling options. We then use the fused estimates of the component outputs to estimate the quantity of interest and the variance of the quantity of interest. Finally, we use global sensitivity analysis to identify key sources of variability in our quantity of interest, which provides the basis for allocating resources to increase the fidelity levels of the most significant contributors to that variability. The full procedure is given below in Algorithm 1, where we also assume we have a quantity of interest variance constraint, which is used to stop the procedure when enough confidence is

achieved.

Algorithm 1: Following the selection of the tth modeling choice, $\mathcal{M}_t$

1: Set the input case to analyze $\mathbf{d}_{\mathcal{M}_t}$ (this could include a system analysis or a system optimization).
2: Quantify model discrepancy for $\mathcal{M}_t$.
3: Calculate $\mathbf{z}_i|\mathbf{d}_{\mathcal{M}_t}$ for $i = 1, \ldots, t-1$.
4: Fuse output information from modeling choices $\mathcal{M}_1, \ldots, \mathcal{M}_t$ to obtain fused estimate $\mathbf{Z}^*$.
5: Estimate quantity of interest statistics, $\mathbb{E}[C|\mathbf{Z}^*]$ and var$(C|\mathbf{Z}^*)$.
6: Check variance constraint satisfaction: If var$(C|\mathbf{Z}^*) \leq \kappa$, STOP.
7: Apportion output variance according to component contributions using global sensitivity analysis.
8: Increase model fidelity of the subsystem with the largest sensitivity index.

The variance of a quantity of interest C, results from uncertainty in model outputs. In our methodology, this uncertainty is due to model discrepancy, which has been elicited from expert opinion. If untrustworthy information is used in quantifying model discrepancy, then it is possible that the algorithm presented here for multifidelity model management could lead to inappropriate model choices as a design or analysis process proceeds. This is due to the sensitivity of the calculation of the senstivities indices on input uncertainties. How sensitive the sensitivity analysis results are to incomplete or untrustworthy information in quantifying input uncertainties is problem specific. For example, for some systems, a discipline may employ a model with a small amount of discrepancy but have a large impact on a particular quantity of interest's variance. In this case, small errors in the discrepancy quantification could lead to large errors in the senstivity index estimates. It may also be the case that for some systems, a discipline employs a model with a large amount of discrepancy but has a negligible impact on the variance of a quantity of interest. In this case, errors in the quantification of discrepancy will not have a large impact on the sensitivity index estimates. The main situation of concern is the case where two disciplines have similar sensitivity indices. Here one needs to be careful because errors in discrepancy estimates could lead to either of the disciplines having the true larger sensitivity index. In this case, incrementing the fidelity of both disciplines may be the most reasonable course of action. If only one discipline may be incremented at a time, then incrementing the more convenient discipline (in terms of model availability, execution time, etc.) is recommended.

4. APPLICATION TO MULTIDISCIPLINARY DESIGN OPTIMIZATION

Our approach is applicable in many settings. Here we show how it can be used to manage models and reduce risk for engineering design decisions. In particular, we focus on a multidisciplinary design optimization (MDO) problem for conceptual (early stage) design. To demonstrate our approach in the MDO context, a wing-sizing problem that could be encountered in the early conceptual design phase of a high altitude, long endurance (HALE) unmanned

aerial vehicle (UAV) is considered. Section 4.1 provides background on multifidelity MDO. The design problem is discussed in Section 4.2 and the results are presented in step-by-step fashion in Section 4.3. For purposes of this demonstration, we assume that the outputs of the disciplinary models are all pairwise independent.

4.1 Multifidelity MDO

MDO is a tool that has been used successfully throughout design processes to enable improvements in the performance of aerospace vehicles, ground vehicles, electrical circuits, computers, and many other products. For example, in the case of an aerospace vehicle, by simultaneously considering the effects of aerodynamics, structures, and controls, MDO can achieve substantially improved performance in metrics such as minimum weight, maximum range, minimum fuel use, etc. It is often the case that the many different disciplines represented in an MDO process will each have several different modeling options available for use. Each of these options is likely to have different levels of computational cost and model fidelity. Multifidelity optimization methods seek to combine performance estimates from the different modeling options, often striving to use inexpensive lower fidelity analyses to accelerate convergence towards the optimum of a high-fidelity design problem.

In existing multifidelity optimization methods, it is common to treat the models as a hierarchy and replace or calibrate low-fidelity information with high-fidelity results [29–35]. For example, Refs. [29] and [30], employ a trust-region based model-management method by scaling or shifting the gradients of the low-fidelity objective function and constraints to match those of a high-fidelity model. In cases where gradients are not available, calibration techniques such as efficient global optimization [31] and surrogate management framework [32] are often employed.

Here we follow our methodology for managing and fusing information from multifidelity models developed in Section 3. Our proposed approach to managing and fusing information leads to a new view of multifidelity MDO. In our approach, rather than treat the models as a hierarchy, we treat the models as individual information sources. By endowing each model with uncertainty in the form of model discrepancy, we are able to maintain confidence in estimates from each model and fuse these estimates rather discard information from lower fidelity models. To implement our methodology in the MDO context, Step 1 of Algorithm 1 becomes the solution of a deterministic

MDO problem,

$$\begin{aligned} \min_{\mathbf{d}_{\mathcal{M}_t}} \quad & c|\mathbf{d}_{\mathcal{M}_t}, \mathcal{M}_t \\ \text{s.t.} \quad & \boldsymbol{h}(\mathbf{d}_{\mathcal{M}_t}) = 0, \\ & \boldsymbol{g}(\mathbf{d}_{\mathcal{M}_t}) \leq 0, \\ & \mathbf{d}_{\mathcal{M}_t} \in \mathcal{D}_{\mathcal{M}_t}, \end{aligned} \tag{27}$$

where $\boldsymbol{h}$ and $\boldsymbol{g}$ are sets of equality and inequality design constraints respectively, and $\mathcal{D}_{\mathcal{M}_t}$ is the set of allowable values of the design variables. The solution of this MDO problem provides us with a design $\mathbf{d}^*$ that minimizes the objective function and satisfues the constraints for the current modeling choice $\mathcal{M}_t$. This step can potentially be carried out with a number of different MDO techniques, such as all-at-once, individual discipline feasible [36], multiple discipline feasible [37], bilevel integrated system synthesis [38], concurrent subspace optimization [39], and analytical target cascading [40]. We leave the decision of how to solve the deterministic MDO problem to the practitioner.

4.2 Wing-sizing problem description

The objective of the conceptual design of the HALE vehicle is to minimize c, the mass of fuel used for a fixed range mission in cruise conditions. The design variables $\mathbf{d}$, are the wing span b, and the aspect ratio AR, which impact both the aircraft takeoff mass and the lift-to-drag ratio. The component outputs $\mathbf{z}$ are the lift and drag coefficients (C_L and C_D respectively) and takeoff mass (m_{TO}). The Breguet range equation calculates the quantity of interest, which here is the mass of fuel used for a fixed range mission. The inputs, outputs, and quantity of interest are summarized in Table 1. The calculation of the lift and drag coefficients and the takeoff mass involves modeling the aerodynamic

TABLE 1: Inputs, component outputs, and quantity of interest for the wing-sizing problem

Methodology quantity	Wing-sizing problem quantity
$\mathbf{d}$	$[\ \mathrm{AR},\ \mathrm{b}]^T$
$\mathbf{z}_{\mathrm{aero}}$	$[\mathrm{C}_L,\ \mathrm{C}_D]^T$
$\mathbf{z}_{\mathrm{structures}}$	$[\mathrm{m}_{TO}]$
c	Mass of fuel used

and structural components of the design. For this problem we have two different models for each discipline, which represent two levels of fidelity for each. These models are referred to as the low- and medium-fidelity aerodynamics and the low- and medium-fidelity structures models.

Both the low- and medium-fidelity aerodynamics models have the same inputs and are used to compute the lift and

drag coefficients of the vehicle; that is, $\mathbf{z}_{\text{aero}} = [C_L, C_D]$. The low-fidelity aerodynamics module assumes a constant value for the coefficient of lift of 0.6, which is representative of typical HALE wing profiles. The medium-fidelity model uses a more advanced technique to compute the coefficient of lift based on lifting line theory [41]. The drag coefficient is calculated in both models as the sum of wing friction, profile, and induced drag multiplied by a factor of 1.3 to account for fuselage and empennage drag. These drag components are calculated using the methods found in Ref. [42].

Both the low- and medium-fidelity structures models also have the same inputs and are used to compute the takeoff mass of the vehicle; that is $\mathbf{z}_{\text{structures}} = [\text{m}_{TO}]$ The low-fidelity model assumes a rectangular wing, while the medium-fidelity model assumes an elliptical wing. For both models, the takeoff mass is the sum of the aircraft body mass without the wing (a fixed parameter), the wing mass, and the fuel mass at takeoff. The fuel volume is assumed to be 50% of the wing volume. The mass of the wing is calculated by sizing the cap and web of the wing's structural box beam to sustain the shear force and bending moment of the wing, which are both functions of the load factor and the aircraft body weight and were calculated using the methods presented in Ref. [43].

4.3 Results

Algorithm 1 is applied to the wing-sizing problem defined in the previous subsection. The results are discussed here on a step-by-step basis through each iteration of the algorithm. As an example, the design goal is taken to be reducing the variance of the quantity of interest estimate to an acceptable level. Here we define an acceptable level to be 50,000 kg^2.

Iteration 1; $\mathcal{M}_1$ = {low-fidelity aerodynamics, low-fidelity structures}

Step 1. The first step in the algorithm in the context of MDO is solving the optimization problem using the lowest fidelity models for both the aerodynamics and structures disciplines. In this work we used an all-at-once formulation solved using sequential quadratic programming. Solving this optimization problem provides us with the design case (inputs) we wish to analyze. Thus, we minimize the mass of fuel used subject to the low-fidelity aerodynamics and structures models, which we denote by $\mathcal{M}_1$, over the possible values of the aspect ratio and span of the wing. The results of this optimization are given in Table 2.

Step 2. The next step is to quantify model discrepancy for $\mathcal{M}_1$ so that we may assess the variance in the quantity of

TABLE 2: Results of Step 1 of the algorithm for the low-fidelity aerodynamics and low-fidelity structures models.

Variable	Deterministic Estimate
AR	26.98
b	34.99 m
C_L	0.600
C_D	0.0166
m_{TO}	8,884 kg
Mass of fuel used	3,544 kg

interest estimate. Our expert stated the low-fidelity aerodynamics and low-fidelity structures models could produce estimates of their respective disciplinary outputs within $\pm 15\%$ of their true values given the design variables. Here it should be noted that multiple outputs from the same discipline (e.g. C_L and C_D from the aerodynamics model) are not required to have the same model discrepancy. The method of mapping this model discrepancy information to a probability distribution discussed in Section 3.1 is used to establish conservative maximum entropy distributions for each disciplinary output as

$$C_L \sim \mathcal{N}(0.6, 0.0081), \tag{28}$$

$$C_D \sim \mathcal{N}(0.0166, 6.22 \times 10^{-6}), \tag{29}$$

$$m_{TO} \sim \mathcal{N}(8884, 1.78 \times 10^{6}), \tag{30}$$

which are shown graphically in Figure 3.

Step 3 and Step 4. These steps of the process are only necessary if more than one model has been used for a given discipline. Since this is the first pass through the algorithm, only one model has been used for both aerodynamics and structures, and thus these steps are unnecessary at this point.

Step 5 and Step 6. For this demonstration, Monte Carlo simulation is used to propagate disciplinary output uncertainty to the quantity of interest estimate, though other techniques, such as using generalized polynomial chaos expansions [44] and quasi-Monte Carlo [45] could also have been used. The Monte Carlo simulation is used to provide samples of the quantity of interest given samples of the discrepancy terms, which are added to the disciplinary outputs of the modeling choice employed. Thus, only one run of each modeling choice is required. The calculation of the quantity of interest for this demonstration requires a negligible amount of time to complete once the disciplinary models have been executed, and thus many thousands of samples could be had cheaply. We assumed convergence

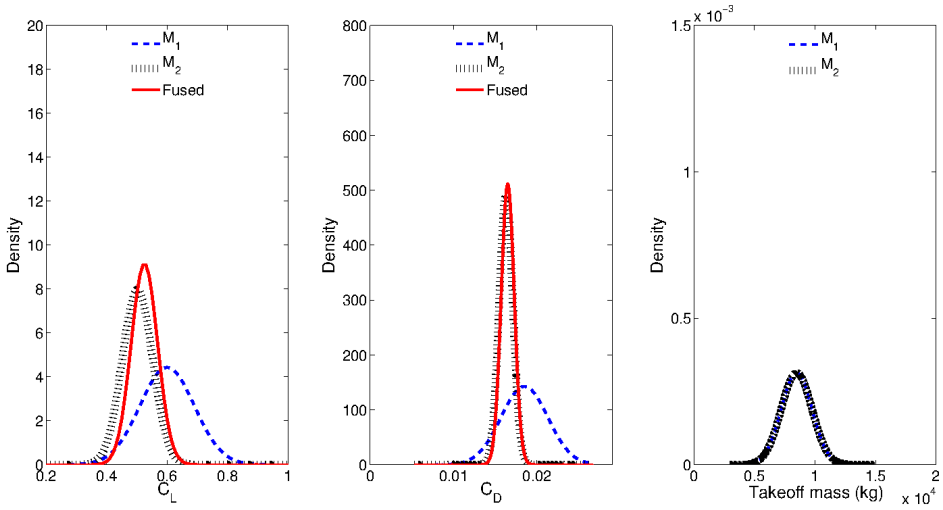

FIG. 3: Maximum entropy distributions of disciplinary outputs derived from model discrepancy information for $\mathcal{M}_1$ and $\mathcal{M}_2$. The aerodynamics estimates from $\mathcal{M}_1$ and $\mathcal{M}_2$ have been fused with the procedure developed in Section 3.4. The $\mathcal{M}_1$ and $\mathcal{M}_2$ structures estimates are identical and are thus not fused.

when the variance of the quantity of interest and the global sensitivity indices varied less than one percent when 1000 new samples are added. Given this method, the mean of the mass of fuel used when estimated with the low-fidelity aerodynamics and low-fidelity structures models is 3,540 kg. The variance of the mass of fuel used is 325,280 kg^2. The variance calculated using the low-fidelity models for both aerodynamics and structures disciplines is greater than the variance constraint of 50,000 kg^2. Thus, we continue the algorithm.

Step 7 and Step 8. Since the variance constraint is not satisfied, it is necessary to apportion the variance between the aerodynamics and structures disciplines to determine which discipline is responsible for most of the variation in the quantity of interest. This is accomplished using global sensitivity analysis discussed in Section 3.2. The analysis reveals that about 66% of the variance is caused by the aerodynamics model, with the remaining 34% being caused by the structures model. This is shown in Figure 4.

Given the results of the variance apportionment, the aerodynamics model is responsible for more of the variance of the quantity of interest and thus the fidelity of the model for the aerodynamics discipline should be increased.

Iteration 2; $\mathcal{M}_2 = \{$medium-fidelity aerodynamics, low-fidelity structures$\}$

Step 1. With the medium-fidelity aerodynamics and low-fidelity structures models in place (denoted by $\mathcal{M}_2$), the

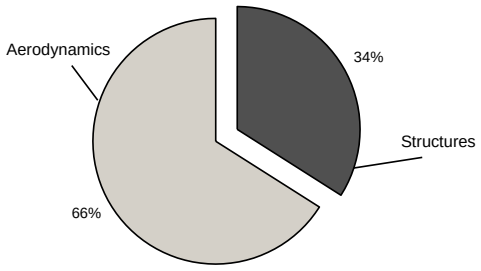

FIG. 4: Quantity of interest variance apportionment between the aerodynamics and structures disciplines for the low-fidelity aerodynamics and low-fidelity structures models.

optimization problem is solved again. The results of this optimization are given in Table 3.

TABLE 3: Results of Step 1 of the algorithm for the medium-fidelity aerodynamics and low-fidelity structures models.

Variable	Deterministic Estimate
AR	20.90
b	29.18 m
C_L	0.502
C_D	0.0163
m_{TO}	8,484 kg
Mass of fuel used	3,490 kg

Step 2. After the optimization problem is solved, the next step is to quantify model discrepancy for $\mathcal{M}_2$ so that we may assess the variance in the quantity of interest estimate. Our expert stated the medium-fidelity aerodynamics model could produce estimates of C_L and C_D within $\pm 10\%$ and $\pm 5\%$ respectively of their true values given the design variables. The method of mapping this model discrepancy information to a probability distribution discussed in Section 3.1 is again used to establish conservative maximum entropy distributions for C_L, C_D and m_{TO} as

$$C_L \sim \mathcal{N}(0.502, 0.0025), \tag{31}$$

$$C_D \sim \mathcal{N}(0.0163, 6.61 \times 10^{-7}), \tag{32}$$

$$m_{TO} \sim \mathcal{N}(8484, 1.62 \times 10^{6}). \tag{33}$$

Note, the takeoff mass distribution has changed as a result of different optimum design variables. These distributions are shown graphically in Figure 3.

Step 3. The third step of the algorithm involves calculating the disciplinary outputs for previously used models using the current optimum values of the design variables. Thus, the lift and drag coefficients must be computed using the low-fidelity aerodynamics model with the design variables set to the values given in Table 3. This results in a lift coefficient of 0.6 and a drag coefficient of 0.0185.

Step 4. Given there are now two estimates of both the lift and drag coefficients (a low and medium-fidelity estimate for each), the next step is to fuse this information together using the procedure developed in Section 3.4 to obtain a better estimate of these disciplinary outputs. For this demonstration, we assume that all models are uncorrelated. This results in the following new estimates of the distributions of C_L and C_D:

$$C_L \sim \mathcal{N}(0.525, 0.0019), \tag{34}$$

$$C_D \sim \mathcal{N}(0.0165, 6.09 \times 10^{-7}). \tag{35}$$

These fused distributions are shown in Figure 3.

Step 5 and Step 6. Using Monte Carlo simulation the mean of the mass of fuel used when estimated with the fused aerodynamics and low-fidelity structures models is 3,456 kg. The variance of the mass of fuel used is 138,370 kg^2. The variance calculated using the fused aerodynamics models and the low-fidelity structures model is greater than the variance constraint of 50,000 kg^2. Thus, we continue the algorithm.

Step 7 and Step 8. Since the variance constraint is not satisfied, it is once again necessary to apportion the variance between the aerodynamics and structures disciplines to determine which discipline is responsible for most of the variation in the quantity of interest estimate. The analysis revealed that about 25% of the remaining variance is caused by the aerodynamics discipline, while 75% is caused by the structures discipline. This is shown in Figure 5.

Given the results of the variance apportionment, the structures model is now responsible for more of the variance of the quantity of interest estimate and thus the fidelity of the structures model should be increased.

Iteration 3; $\mathcal{M}_3$ = {medium-fidelity aerodynamics, medium-fidelity structures}

Step 1. With the medium-fidelity aerodynamics and medium-fidelity structures models in place (denoted by $\mathcal{M}_3$), the

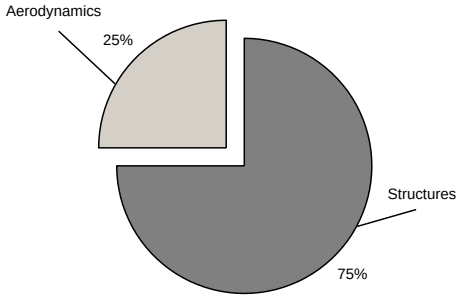

FIG. 5: Quantity of interest estimate variance apportionment between the aerodynamics and structures disciplines for the fused aerodynamics and low-fidelity structures models.

optimization problem is solved again. The results of this optimization are given in Table 4.

TABLE 4: Results of Step 1 of the algorithm for the medium-fidelity aerodynamics and medium-fidelity structures models.

Variable	Deterministic Estimate
AR	19.34
b	27.99 m
C_L	0.497
C_D	0.0166
m_{TO}	8,464 kg
Mass of fuel used	3,539 kg

Step 2. With the optimization problem solved, the next step is to quantify model discrepancy for $\mathcal{M}_3$ so that we may once again assess the variance in the quantity of interest estimate. Our expert stated the medium-fidelity structures model could produce an estimate of takeoff mass within $\pm 5\%$ of its true values given the design variables. The method of mapping this model discrepancy information to a probability distribution discussed in Section 3.1 is again used to establish conservative maximum entropy distributions for C_L, C_D and m_{TO} as

$$C_L \sim \mathcal{N}(0.497, 0.0025), \tag{36}$$

$$C_D \sim \mathcal{N}(0.0166, 6.87 \times 10^{-7}), \tag{37}$$

$$m_{TO} \sim \mathcal{N}(8464, 1.79 \times 10^5). \tag{38}$$

Note, the lift and drag coefficient distributions have changed as a result of different optimum design variables. These

distributions are shown graphically in Figure 6.

Step 3. In order to fuse the low and medium disciplinary output estimates from both the aerodynamics and structures disciplines, the disciplinary outputs for the low-fidelity models must be computed using the current optimum values of the design variables. The low-fidelity disciplinary outputs of the aerodynamics model using the current optimum design variables are $C_L = 0.6$ and $C_D = 0.0191$. The low-fidelity disciplinary output of the structures model using the current optimum design variables is $\mathrm{m}_{TO} = 8{,}287$ kg.

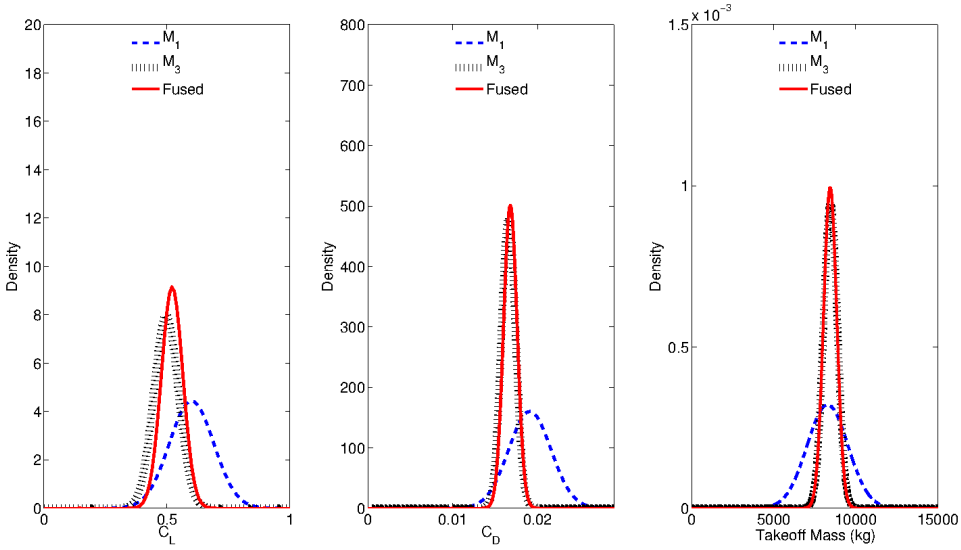

FIG. 6: Maximum entropy distributions of disciplinary outputs derived from model discrepancy information for $\mathcal{M}_1$ and $\mathcal{M}_3$. The estimates from $\mathcal{M}_1$ and $\mathcal{M}_3$ have been fused with the procedure developed in Section 3.4.

Step 4. Given there are now two estimates of all of the disciplinary outputs, the next step is to fuse this information together using the approach discussed in Section 3.4 to obtain better estimates. This results in the following new estimates of the distributions of C_L, C_D, and m_{TO}:

$$C_L \sim \mathcal{N}(0.521, 0.0019), \tag{39}$$

$$C_D \sim \mathcal{N}(0.0168, 6.34 \times 10^{-7}), \tag{40}$$

$$\mathrm{m}_{TO} \sim \mathcal{N}(8446, 1.61 \times 10^{5}). \tag{41}$$

These distributions are shown in Figure 6, along with the previous estimates of the respective distributions.

Step 5 and Step 6. Using Monte Carlo simulation the mean of the mass of fuel used when estimated with the fused aerodynamics and structures models is 3,517 kg. The variance of the mass of fuel used is 39,014 kg^2. This variance is less than the variance constraint of 50,000 kg^2. Thus, we exit the algorithm.

The MDO problem we have considered here could be encountered in the early conceptual phases of a high altitude, long endurance aerospace vehicle. Application of the approach to this design problem results in risk mitigation in the form of an 88% reduction in the initial variance of the quantity of interest estimate. This is achieved via a systematic means of fusing information from various models and managing model fidelity throughout the design process through the application of the powerful tools of Bayesian inference and global sensitivity analysis.

5. CONCLUSIONS

Model discrepancy poses a serious risk to the critical decisions made using the outputs of computer models that support analysis and design. In many cases, achieving truly high-fidelity simulation capabilities may be unachievable; instead, we must accept the inadequacy of our models and invest in strategies to account for it. The methodology proposed here is a first step in this direction, using a probabilistic approach to endow all analysis models with quantified uncertainties. These uncertainties are explicitly maintained and propagated through the design and synthesis process, resulting in quantified uncertainties on the output estimates of quantities of interest. These output uncertainties provide rigorous guidance to manage multifidelity models, through identification of particular disciplines or subsystems that contribute unacceptably high levels of uncertainty, and also provide design/analysis risk assessment, through quantified uncertainty bands on simulation outputs. The proposed global sensitivity analysis approach to identifying contributors to output variance is broadly applicable, while the proposed approaches to represent model discrepancy and to fuse multifidelity information are limited to Gaussian distributions of uncertainty in model component outputs. Extending these approaches to handle more general distributions is an important area of future work.

ACKNOWLEDGMENTS

This work was supported by the AFOSR STTR Program, Program Manager Dr. Fahroo, Technical Monitor Dr. Camberos, under contract FA9550-09-C-0128. The authors also acknowledge the contributions of O. Toupet and Aurora Flight Sciences, Inc. in setting up the example problem.

REFERENCES

1. Deyst, J. The application of estimation theory to managing risk in product developments. Proceedings of the 21st Digital Avionics Systems Conference, Volume 1. pp. 4A3-1-4A3-12, 2002.
2. Bauer, S., Liedl, R., and Sauter, M., Modeling of karst development considering conduit-matrix exchange flow, calibration and reliability in groundwater modeling: coping with uncertainty, *Int. Assoc. Hydrol. Sci.*, 265:10–15, 2000.
3. Cao, Y., Gunzburger, M., Hua, F., , and Wang, X., Analysis and finite element approximation of a coupled, continuum pipe-flow/Darcy model for flow in porous media with embedded conduits, *Numer. Meth. PDE*, 2011, to appear.
4. Cao, Y., Gunzburger, M., Hua, F., , and Wang, X., Coupled Stokes-Darcy model with Beavers-Joseph interface boundary condition, *Comm. Math. Sci.*, 8:1–25, 2010.
5. Cao, Y., Gunzburger, M., Hu, X., Hua, F., Wang, X., , and Zhao, W., Finite element approximations for Stokes-Darcy flow with Beavers-Joseph interface conditions, *SIAM J. Numer. Anal.*, 47:4239–4256, 2010.
6. Harvey, D., Gregory, J., Hoffert, M., Jain, A., Lal, M., Leemans, R., Raper, S., and de Wolde, T. W. J. An introduction to simple climate models used in the IPCC second assessment report. IPCC Technical Paper 2, 1997.
7. Randall, D., wood, R., Bony, S., Colman, R., Fichefet, T., Fyfe, J., Kattsov, V., Pitman, A., Shulka, J., Srinivasan, J., Stouffer, , Sumi, A., and Taylor, K. Climate models and their evaluation. Climate Change 2007: The Physical Basis. Contribution of Working Group 1 to the Fourth Assessment Report of the Intergovernmental Panel on Climate Change, 2007.
8. Kennedy, M. and O'Hagan, A., Bayesian calibration of computer models, *J.R. Statist. Soc. B*, 63(3):425–464, 2001.
9. Kennedy, M., O'Hagan, A., and Higgins, N., Bayesian analysis of computer code outputs, *Quantitative Methods for Current Environmental Issues*, pp. 227–243, 2002.
10. Goldstein, M. and Rougier, J., Reified Bayesian modelling and inference for physical systems, *Journal of Statistical Planning and Inference*, 139(3):1221–1239, 2006.
11. Park, I., Amarchinta, H., and Grandhi, R., A Bayesian approach for quantification of model uncertainty, *Reliability Engineering and System Safety*, 95:777–785, 2010.

12. Link, W. and Barker, R., Model weights and the foundations of multimodel inference, *Ecology*, 87(10):2626–2635, 2006.

13. Zio, E. and Apostolakis, G., Two methods for the structured assessment of model uncertainty by experts in performance assessments of radioactive waste repositories, *Reliability Engineering and System Safety*, 54(2-3):225–241, 1996.

14. Reinert, J. and Apostolakis, G., Including model uncertainty in risk-informed decision making, *Annals of Nuclear Energy*, 33(4):354–369, 2006.

15. Burnham, K. and Anderson, D., *Model Selection and and Multi-model Inference: A Practical Guide Information-theoretic Approach*, Springer-Verlag, New York, NY, 2 edition, 2002.

16. Leamer, E., *Specification Searches: Ad Hoc Inference with Nonexperimental Data*, John Wiley & Sons, New York, NY, 1978.

17. Rasmussen, N. Reactor safety study: An assessment of accident risks in u.s. power plants. WASH-1400-NUREG 74/014, U.S. Nuclear Regulatory Commission, 1975.

18. Elton, E. and Gruber, M., Modern portfolio theory, 1950 to date, *Journal of Banking & Finance*, 21:1743–1759, 1997.

19. Jaynes, E., Information theory and statistical mechanics, *The Physical Review*, 106(4):620–630, 1957.

20. Jaynes, E., *Probability Theory: The Logic of Science*, Cambridge University Press, Cambridge, United Kingdom; New York, 2003.

21. Babuscia, A. and Cheung, K., Statistical risk estimation for communication system design: a preliminary look, *The Interplanetary Network Progress Report*, 42-188:1–33, 2012.

22. Rabitz, H. and Alis, O., General foundations of high-dimensional model representations, *Journal of Mathematical Chemistry*, 25:197–233, 1999.

23. Ma, X. and Zabaras, N., An adaptive high-dimensional stochastic model representation technique for the solution of stochastic partial differential equations, *Journal of Computational Physics*, 229:3884–3915, 2010.

24. Saltelli, A., Ratto, M., Andres, T., Campolongo, F., Cariboni, J., Gatelli, D., Saisana, M., and Tarantola, S., *Global Sensitivity Analysis: The Primer*, John Wiley & Sons, Ltd., West Sussex, England, 2008.

25. Saltelli, A., Tarantola, S., and Chan, K., A quantitative model independent method for global sensitivity analysis of model output, *Technometrics*, 41:39–56, 1999.

26. Sudret, B., Global sensitivity analysis using polynomial chaos expansions, *Reliability Engineering and System Safety*, 93(7):964–979, 2008.

27. Buzzard, G. and Xiu, D., Variance-based global sensitivity analysis via sparse grid interpolation and cubature, *Comm. Comput. Phys.*, 9(3):542–567, 2011.

28. Winkler, R., Combining probability distributions from dependent information sources, *Management Science*, 27(4):479–488, 1981.

29. Alexandrov, N., Lewis, R., Gumbert, C., Green, L., and Newman, P. Optimization with variable-fidelity models applied to wing design. NASA Tech. Rep. CR-209826, December 1999.

30. Alexandrov, N., Lewis, R., Gumbert, C., Green, L., and Newman, P., Approximation and model management in aerodynamic optimization with variable-fidelity models, *AIAA Journal*, 38(6):1093–1101, November-December 2001.

31. Jones, D., Schonlau, M., and Welch, W., Efficient global optimization of expensive black-box functions, *Journal of Global Optimization*, 13:455–492, 1998.

32. Booker, A., Dennis, J., Frank, P., Serafini, D., Torczon, V., and Trosset, M., A rigorous framework for optimization of expensive functions by surrogates, *Structural Optimization*, 17(1):1–13, February 1999.

33. Jones, D., A taxonomy of global optimization methods based on response surfaces, *Journal of Global Optimization*, 21:345–383, 2001.

34. Sasena, M., Papalambros, P., and Goovaerts, P., Exploration of metamodeling sampling criteria for constrained global optimization, *Engineering Optimization*, 34(3):263–278, 2002.

35. Rajnarayan, D., Haas, A., and Kroo, I. A multifidelity gradient-free optimization method and application to aerodynamic design. 12th AIAA/ISSMO Multidisciplinary Analysis and Optimization Conference, AIAA-2008-6020, Victoria, British Columbia, September 10-12, 2008.

36. Cramer, E., Frank, P., Shubin, G., Dennis, J., and Lewis, R. On alternative problem formulation for multidisciplinary optimization. In Proceedings of the 4th AIAA/USAF/NASA/OAI Symposium on Multidisciplinary Analysis and Optimization, AIAA-92-4752, 1992.

37. Kodiyalam, S. and Sobieszczanski-Sobieski, J., Multidisciplinary design optimization: Some formal methods, framework requirements and application to vehicle design, *Int J Vehicle Design*, 25:3–32, 2001.

38. Sobieszczanski-Sobieski, J., Agte, J., and Jr., R. S., Bilevel integrated system synthesis, *AIAA Journal*,

38(1):164–172, 2000.

39. Sobieszczanski-Sobieski, J. Optimization by decomposition: A step from hierarchic to non-hierarchic systems. In Proceedings of the 2nd NASA/Air Force Symposium on Recent Advances in Multidisciplinary Analysis and Optimization, NASA-CP-3031, 1988.

40. Kim, H., Rideout, D., Papalambros, P., and Stein, J., Analytical target cascading in automotive vehicle design, *J Mech Des*, 125:481–489, 2003.

41. Anderson Jr., J. *Fundamentals of Aerodynamics*, chapter 5, pp. 360–367. McGraw-Hill, New York, NY, 3 edition, 2001.

42. Raymer, D. *Aircraft Design: A Conceptual Approach*, chapter 12, pp. 340–366. American Institute of Aeronautics and Astronautics, Inc., Reston, VA, 3 edition, 1999.

43. Young, W. *Roark's Formulas for Stress and Strain*, chapter 7,8, pp. 95–243. McGraw-Hill, New York, NY, 6 edition, 1989.

44. Xiu, D. and Karniadakis, G., The Wiener-Askey polynomial chaos for stochastic differential equations, *SIAM J. Sci Comput.*, 24(2):619–644, 2002.

45. Niederreiter, H., *Random Number Generation and Quasi-Monte Carlo Methods*, Society for Industrial and Applied Mathematics, Philadelphia, Pennsylvania, 1992.